17th World Conference on Earthquake Engineering, 17WCEE
Sendai, Japan - September 13th to 18th 2020
Paper N° C000147
Registration Code: S-A00695

RANKING OF PULSE-LIKE GROUND MOTIONS

C. Frau[(1)], M. Tornello[(2)], S. Panella[(3)]

[(1)] *Researcher, Regional Mendoza, National Technologic University (Argentina), cdfrau@frm.utn.edu.ar*
[(2)] *Researcher, Regional Mendoza, National Technologic University (Argentina), mtornell@frm.utn.edu.ar*
[(3)] *Researcher, Regional Mendoza, National Technologic University (Argentina), spanellal@frm.utn.edu.ar*

Abstract

Near-fault seismic ground motions are frequently characterized by intense velocity and displacement pulses of relatively long periods that clearly distinguish them from typical far-field ground motions. Intense velocity pulse motions can affect adversely the seismic performance of structures. In response to the realization of the importance of near-fault motions on structural performance, a number of studies have been directed to developing procedures for the identification of ground motions containing velocity pulses; these procedures classify ground motions as yes/no (pulse or non-pulse). The procedure proposed by Panella, Tornello, and Frau to identify pulse-like ground motions is based on the parameter called "development length of velocity time history". It classifies ground motions in pulse or non-pulse too, but besides that, it is able to assess the level of impulsivity of them. In this work, we present a ranking of pulse-like ground motions based on the severity of the pulses. This paper may be a help to an adequate selection of records that are used to analyze structures in near-fault regions. The study ends with an analysis of the regions in the acceleration response spectra where they are affected for the velocity pulses.

Keywords: near-fault; pulse-like ground motions; development length of velocity; ranking of ground motions

1. Introduction

When a fault ruptures toward a site, a rupture velocity slightly slower than the shear wave velocity produces an accumulation of seismic energy released during rupture [1-3]; this generally results in a large pulse in the velocity-time series. Thus, near-fault seismic ground motions are frequently characterized by intense velocity and displacement pulses of relatively long periods that clearly distinguish them from typical far-field ground motions. Intense velocity pulse motions can affect adversely the seismic performance of structures [4-10].

In response to the realization of the importance of near-fault motions on structural performance, a number of studies have been directed to developing predictive relationships for parameters that characterize this special type of ground motions in the near-fault zone [11-13]. Bray and Rodriguez-Marek [14] identified key parameters in the characterization of forward-directivity pulse motions including amplitude (PGV), velocity pulse period, and a number of significant cycles. However, Rupakhety and Sigbjörnsson [15] found that equivalent pulses often used to characterize the structural response of tall buildings to near-fault ground motions underestimate the peak inter-story drift.

Following the same objective, other researchers assembled sets of pulse-like or near-fault ground motion, but these sets were selected using different criteria. Somerville, Mavroeidis and Papageorgiou, Bray and Rodriguez-Marek, Cox and Scott, and Fu and Menon [2,13,14,16,17] prepared lists of near-fault records regarded as having strong ground motion pulses. Baker [18] and Shahi and Baker [19] developed a method for quantitatively identifying ground motions containing strong velocity pulses, such as those caused by near-fault directivity. The approach uses wavelet analysis to extract the largest velocity pulse from given ground motion. The size of the extracted pulse relative to the original ground motion is used to develop a quantitative criterion for classifying a ground motion as "pulse-like". The criterion was calibrated by using a training data set of manually classified ground motions.

Khanse and Lui [20] present a methodology for identifying earthquake pulses. Because directivity effects are most significant for frequencies of less than 1.67 Hz (i.e., a period longer than 0.6 seconds), this criterion is used in his study to identify pulse characteristics. Hayden et al. [21] developed a quantitative scheme to classify near-fault motions as pulse or non-pulse. This scheme involves filtering the record, calculating several parameters at all orientations, followed by scoring motions based on two key ground motion parameters related to ground velocity: the difference between two successive peaks for different orientations and the square of the normalized cumulative velocity. Mukhopadhyay and Gupta [22] state that the pulse-like movement may be visually identified due to the presence of a large-amplitude pulse, long period, and significant energy content in the history of ground velocities. Zhai et al. [23] propose a quantitative method based on energy to assess pulse-like movements. Maniatakis et al. [24] performed a comparison between Greek records and well-known international near-source records from small, moderate and strong earthquakes.

In general, the different criteria for pulse-like record classification resorts to a visual control of results through direct observation of record traces [18-22-23]. Thus, the observation of the velocity record trace is an effective tool for classification, and so the shape adopted by the velocity history trace is a sign of its impulsive character, despite being qualitative and keeping a certain degree of subjectivity. In addition, in the procedures developed so far to identify pulse-type records, a certain kind of operational complexity makes it difficult to be used by non-specialists. Therefore, for the identification of future records, it may be necessary to resort to the proposers of such procedures, so that they perform the classification correctly.

Panella et al [25] developed a new methodology to identify pulse-like ground motions using an impulsivity idex, obtained from ground velocity time history. The procedure, based on a new parameter called “development length of velocity”, is simple, efficient, and of low computational cost. It is easily

reproducible and captures the criterion of visual classification in a quantitative fashion. The impulsivity index allows for a classification of pulse-like strong motions at different ranges, which helps to consider different impulsivity levels to use in structural analysis. For sites near-fault, it is recommended to use pulse-like ground motions e.g. ASCE 7. These ground motions are chosen from a pulse or non-pulse classification, they do not consider levels of impulsivity. A site within 5 km of an active fault is different from another site at 20 km from the fault. In this work, we intend to present a ranking of pulse-like ground motions with different levels of impulsivity. Then, a procedure to select ground motions is developed. This procedure takes into account the seismic magnitude and fault distance to choose the appropriate level of impulsivity in the records.

2. Ranking of pulse-like ground motions

2.1. Pulse-like ground motions classification

Departing from a velocity time history of ground motion, Panella et al [25] defined a new parameter, the "developed length of velocity" *Ldv* as the length reached by the trace of velocity records as if it were "extended" like a string (Eq. 1).

$$Ld_v = \sum_{i=1}^{n} (\sqrt{(\Delta t)^2 + (\Delta v_i)^2}) \quad (1)$$

where Δt is the time lapse of the record between two successive points *t(i+1)* - *t(i)* in *s*, Δvi are velocity increments between *t(i)* and *t(i+1)* in cm/s, and *n* is the number of samples in the series... Given the binary character of the target classification (pulse-like or non-pulse) and enough data availability, a binary logistic regression was used to classify the records. To obtain the regression, the parameters *Ldv* and *PGV* (Peak Ground Velocity) were used. The logistic regression proved the following predictive equation for the Impulsivity Index by Regression (IP_R).

$$IP_R = \frac{1}{1+e^{(5-0.45PGV+0.01Ldv)}} \quad (2)$$

The Impulsivity Index by Regression takes values between 0 and 1. A ground motion qualifies as pulse type if its IP_R is higher than 0.7 and its *PGV* is higher than 30 cm/s. Below 0.7 the record is non-pulse. It is well-known that several researchers have established as an excluding condition to classify a record as pulse-type that *PGV* should reach a minimum of 30 cm/s [18, 23]. Even though this value is not adequately justified, it imposes a minimum to the power of the pulse for a time velocity series to be classified as pulse-type. The impulsivity level is defined with an indicator based on the development length of velocity and PGV; the "Impulsivity Index" *IP* is as follows:

$$IP = \frac{Ldv}{PGV} \quad (4)$$

The definition of *Ldv* captures in a simple and efficient way the impulsive aspect visually detected in a velocity time series. A relatively low *Ldv* value represents an impulsive character, whereas a high *Ldv* value represents a non-pulse or vibratory character. Pulse amplitude also plays an important role: high *PGV*s reveal the presence of at least one pulse, whereas low *PGV*s "dilute" pulses. In this way, a combination of low Ldv values and high *PGV* leads to small *IP*s suggesting an impulsive character, while the opposite is the manifestation of a non-pulse character. A low *PGV* leads to an increase in *IP*, thus moving the record away from the pulse-type category. The opposite happens if *PGV* is high, but the velocity trace has a greater length *Ldv*. In summary, the lower the IP, the more impulsive the record and, conversely, the higher the IP, the less impulsive the record shall be. Once a record is identified as pulse-type by *IPr*, ranks can be established using the value taken by *IP* to classify ground motions into three impulsivity levels: high, medium or moderate,

and low (see Table 1). Records with *IP* higher than 35 have very low impulsivity. However, *IP* could be used as a classification parameter, where IP=35 divides between pulse and non-pulse.

Table 1 – Classification proposed for different impulsivity levels

Impulsivity Index IP	Impulsivity Level
IP ≤ 12	High (H)
12 < IP ≤ 20	Medium or Moderate (M)
20 < IP ≤ 35	Low (L)

2.2. Database and Rankingof pulse-like ground motions

A database with 1021 records was analyzed, with each record containing two horizontal components that complete 2042 acceleration time histories. The seismic records used correspond to 112 earthquakes in different parts of the world with a moment magnitude between 5.5 and 7.9. Strong motions have a Joyner-Boore distance less than 30 km (RJB_{DIS}<30km). Out of a total of 2042 components analyzed, it was found that out of 455 records classified as pulse-type through IP_R, 41 (9.0%) have $IP \leq 12$, 188 (41.3%) have $12 < IP \leq 20$, and 226 (49.7%) have $20 < IP \leq 35$. Thus, the classification allows choosing records of different impulsivity levels for structural analyses according to the procedure that we describe in the next section [25].

Whit the results found, we have made a ranking of pulse-like ground motions. From high to low impulsivity. Appendix 1 contains the data corresponding to the set of records classified as pulse-type. It shows the ranking of records from high impulsivity (H) passing for moderate impulsivity (M) to low impulsivity (L). Distance to the fault, seismic magnitude, and other parameters are indicated too. Fig. 1 shows two cases: high and low impulsivity.

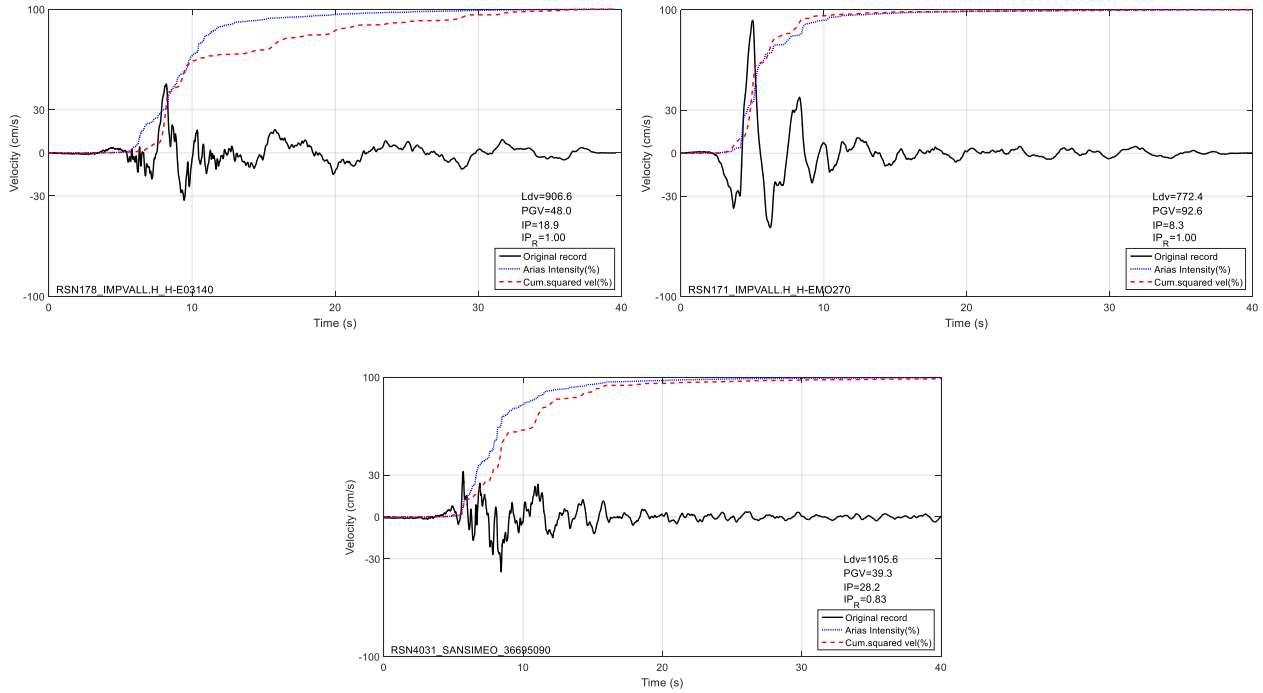

Fig. 1. Records with high (top-left), moderate (top-right) and low (bottom) impulsivity.

3. Procedure to select pulse-like ground motions

For developing the procedure to select records pulse-like and use them in structural analysis, we made a study on the results found for Panella et al [25]. We have chosen three parameters: a) level impulsivity, b) seismic magnitude and c) distance from the site to the fault. With these parameters, we have made a matrix to select the appropriate records to use them in structural analysis.

3.1. Impulsivity level

As it was explained in section 2, the records like-pulse are classified into three levels: high (H), medium or moderate (M), and low (L). A table with the main characteristics is presented in Appendix 1.

3.2. Distance influence

To analyze the influence of the distance from the site to the fault on the level impulsivity, in Fig. 2 it is shown the fault distance versus the seismic magnitude Mw. Each figure is for the different impulsivity levels: high (top), moderate (center) and low (bottom). It is observed that the records with high impulsivity (H) are mainly concentrated on a short distance. A high density of records (H) appears for a distance less than 15 km. It is noticed that records with low impulsivity (L) are very frequent to near fault distance.

When we look at the representation for moderate impulsivity, we can see that much of the records are to distance less 25 km. It is important to take into account that while data cover distances up to 30 km, directivity effects can get up to 50 km [1-2].

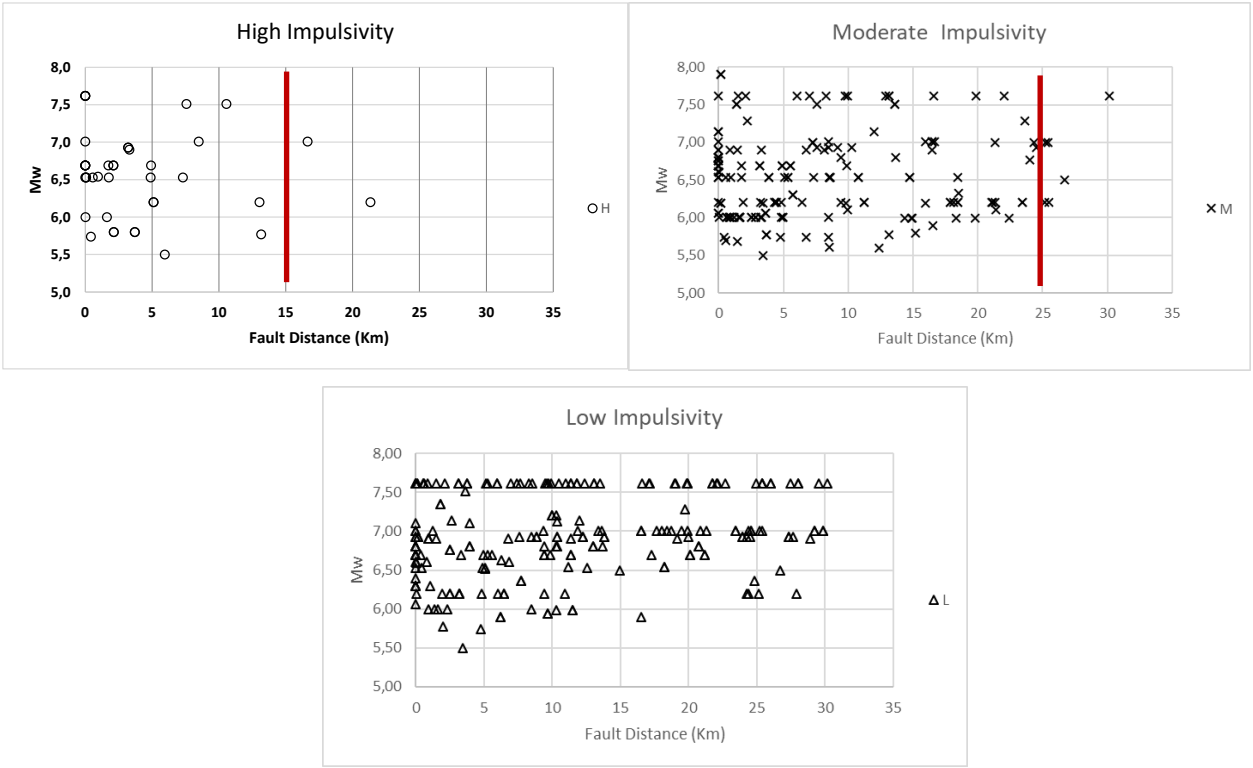

Fig. 2. Fault distance versus the seismic magnitude Mw for different impulsivity levels. High (top,), moderate (center) and low (bottom).

From the distribution of the data, we defined three zones to relate the fault distance with the level impulsivity. It is admitted that it may have some of subjectivity in the limits proposed, but those limits respond to conservative criteria and in this way do not underestimate the seismic demand in near fault regions. The classification and the limits are shown in Table 2.

Table 2 – Classification proposed for the fault distance

Zone	Fault Distance
1. High (H)	FD ≤ 15 km
2. Medium or Moderate (M)	15 < FD ≤ 25
3. Low (L)	25 < FD ≤ 50

3.3. Magnitude influence

In general, each earthquake has many records in different stations, some earthquakes have more than 20 records like-pulse. The influence of the seismic magnitude on the level impulsivity is assessed by the record with higher level impulsivity in each earthquake. We have represented these cases in Fig. 3. In it, we show the seismic magnitude (horizontal axis) versus the level impulsivity (vertical axis). We have plotted two horizontal lines in correspondence with the limits between high, medium and low impulsivity (*IP*=12 and *IP*=20). It is observed that the magnitude *Mw*=6.0 separates the datas in two zones. One with Mw<6.0 where there are not points with *IP*<12 and another zone with *Mw*>6.0 points appear with *IP*<12. There are not points with *Mw*<5.5 and *IP*<20.

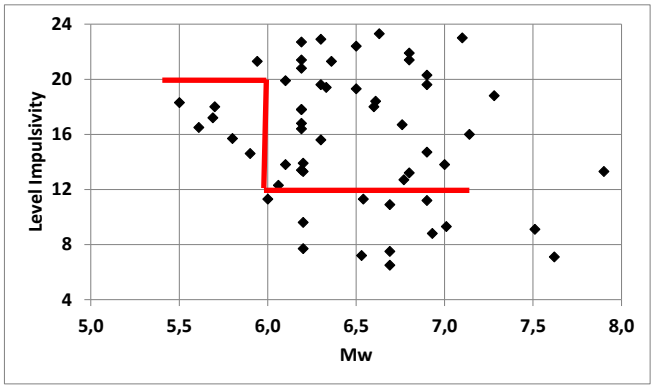

Fig. 3. Relationship between Mw and IP for records with higher IP in each earthquake.

Acording to what was said, we propose to assign high impulsivity (H) to magnitudes greater to 6.0, moderate impulsivity (M) to magnitudes between 6.0 and 5.5, and low impulsivity (L) to magnitudes lower 5.5. This criterion is showed in the Table 3.

Table 3 – Classification for Magnitude and Level Impulsivity

Magnitude Mw	Level Impulsivity
Mw ≥ 6.0	High (H)
5.5 ≤ Mw < 6.0	Medium or Moderate (M)
Mw < 5.5	Low (L)

3.4. Matrix to select ground motions

The interaction between the seismic magnitude and de fault distance is shown in the Fig. 4. In it, all impusive records are represented (H, M and L), and the limits to magnitudes and distances according to de sections 3.2 and 3.3. When Tables 2 and 3 are combined, different kind of iteractions appear: a) strong interactions: (HxH = H_0), (MxM = M_0) or (LxL = L_0) and b) weak interactions: (HxM=MxH = H1), (HxL=LxH = M1), (MxL=LxM=L1); where H is High and L is Low. The subscript zero indicates strong interactions and the subscript one (1) indicates weak interactions. Thus, we can choose different levels of impulsivity within the same category.

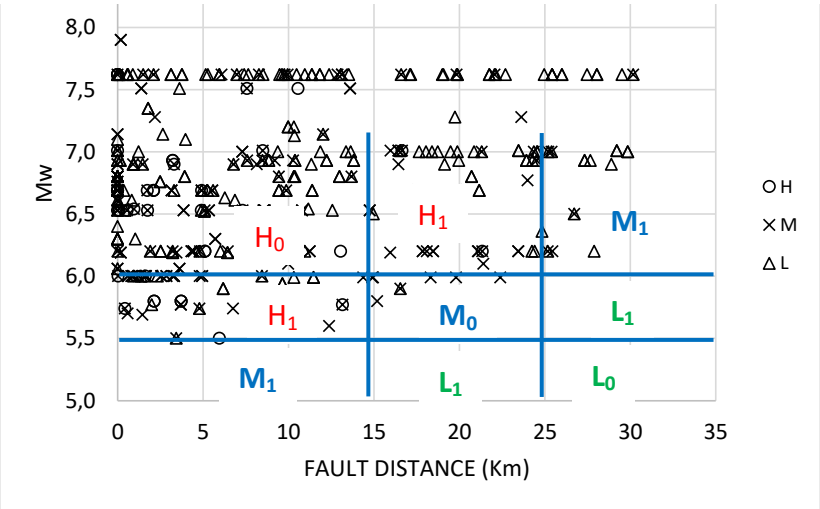

Fig. 4. Interaction between the seismic magnitude and the fault distance

With this classification we organized a matrix to select proper impulsive records to use in structural analysis (Table 4). This matrix combines the key parameters studied: the level impulsivity, seismic magnitude and fault distance. This matrix together with the ranking of strong motions pulse-like will allow designers to make more realistic analysis for structures that take place in near-fault regions.

Table 4 – Selection matrix of records to structural analysis

SELECTION MATRIX		FAULT DISTANCE (km)		
		FD ≤ 15	15 < FD ≤ 25	25 < FD ≤ 50
SEISMIC MAGNITUDE	Mw ≥ 6.0	H_0	H_1	M_1
	5.5 ≤ Mw < 6.0	H_1	M_0	L_1
	Mw < 5.5	M_1	L_1	L_0

4. Conclusions

A methodology to identify pulse-like ground motions was used to organize a ranking of records according to the level impulsivity. The records are classified in three levels: high (H), moderate (M) and low (L).

A procedure to select impulsive records to structural analysis in near-fault regions was developed. It uses three parameter: level impulsivity, seismic magnitude and distance from the site to fault.

The result is a matrix that allows an appropriate selection of ground motions pulse-like in an easy and fast way. Records can be chosen from the ranking proposed in the Appendix 1.

5. Acknowledgements

The authors wish to express their gratitude to the Doctoral Scholarships Program of the Department of Science and Technology of National Technological University (Argentina) and to the Regional Center of Technological Development for Construction, Seismology and Earthquake Engineering (CeReDeTeC) for their support for the present study.

6. References

[1] Somerville PG, Smith NF, Graves RW, Abrahamson NA. Modification of empirical strong ground motion attenuation relations to include the amplitude and duration effects of rupture directivity. Seismological Research Letters 1997; 68:199–222.
[2] Somerville, PG., Magnitude scaling of the near fault rupture directivity pulse, Phys. Earth Planet 2003. Interiors 137, no. 1, 12.
[3] Spudich P, and Chiou, BSJ. Directivity in NGA earthquake ground motions: Analysis using isochrone theory. Earthquake Spectra 2008. 24:1, 279-298
[4] Bertero VV, Mahin SA, Herrera RA. Aseismic design implications of San Fernando earthquake records. Earthquake Engng. Struct. 1978. Dyn. 6(1), 31-42
[5] Anderson JC, Bertero VV. Uncertainties in establishing design earthquakes. J. Struct.Eng. 1987, ASCE 113(8), 1709-1724.
[6] Hall JF, Heaton TH, Halling MW, Wald DJ. Near-source ground motion and its effects on flexible buildings. Earthq. Spectra 1995. 11, no. 4, 569–605.
[7] Naeim, F. On seismic design implications of the 1994 Northridge Earthquake records, Earthquake Spectra 1995. 11, 91–109.
[8] Iwan, WD. Drift spectrum: measure of demand for earthquake ground motions. J. Struct. Eng. 1997. 123, no. 4, 397–404.
[9] Alavi B, Krawinkler H. Effects of near-fault ground motions on frame structures. Technical Report Blume Center Report 138.2001, Stanford, California.
[10] Chopra AK, Chintanapakdee C. Comparing response of SDF systems to near- fault and far-fault earthquake motions in the context of spectral regions. Earthquake Engineering & Structural Dynamics 2001; 30:1769–89.
[11] Alavi B, Krawinkler H. Consideration of near-fault ground motion effects in seismic design. Proceedings. 12th World Conf. on Earthquake Engineering 2000, Auckland, New Zealand.
[12] Somerville PG. Magnitude scaling of near fault ground motion. Proc. Int. Workshop on Annual Commemoration of Chi-Chi earthquake 2000. Vol. 1, 59-70.
[13] Mavroeidis GP, Papageorgiou AS. A mathematical representation of near-fault ground motions. Bulletin of the Seismological Society of America 2003; 93(3):1099 –1131.
[14] Bray J, Rodriguez-Marek A. Characterization of forward-directivity ground motions in the near-fault region. Soil Dynamics and Earthquake Engineering 2004. 24, 815-828. Elsevier Ltd.
[15] Rupakhety R, Sigbjörnsson R. Can Simple Pulses Adequately Represent Near-Fault Ground Motions? Journal of Earthquake Engineering 2011. 15:8, 1260-1272
[16] Cox KE, Ashford S A. Characterization of large velocity pulses for laboratory testing. Pacific Earthquake Engineering Research Center, University of California at Berkeley, Berkeley, California, 60, 2002.
[17] Fu Q, Menun C. Seismic-environment-based simulation of near-fault ground motions. Proceedings of the 13th World Conference on Earthquake Engineering 2004. Vancouver, Canada, 15 p.
[18] Baker J.W. Quantitative classification of near-fault ground motions using wavelet analysis. Bulletin of the Seismological Society of America 2007; 97:1486–501.
[19] Shahi, S.K. and Baker, J.W. (2014). "An efficient algorithm to identify strong velocity pulses in multi-component ground motions." Bulletin of the Seismological Society of America, 104(5), 2456-2466.
[20] Khanse AC, Lui EM. Identification and analysis of pulse effects in near fault ground motions. In: Proceedings of the 14th World Conference on Earthquake Engineering, Beijing, China, Paper No. 02-0015; 2008 (on CD).
[21] Hayden C.P., Bray J.D., N.A. Abrahamson N.A., Acevedo-Cabrera A.L. Selection of Near-Fault Pulse Motions for Use in Design. In: Proceedings of the 15th World Conference on Earthquake Engineering, Lisboa, Portugal, Paper No. 3752; 2012 (on CD).
[22] Mukhopadhyay S, Gupta VK. Directivity pulses in near-fault ground motions-I: Identification, extraction and modeling. Soil Dynamics and Earthquake Engineering 2013; 50: 1-15.
[23] Zhai C., Chang Z., Li S., Chen Z., Xie L. Quantitative Identification of Near-Fault Pulse-Like Ground Motions Based on Energy. Bulletin of the Seismological Society of America 2013; 103:5, 2591-2603.
[24] Maniatakis ChA, Taflampas IM, Spyrakos C.C. Identification of near-fault earthquake record Characteristics. In: Proceedings of the 14th World Conference on Earthquake Engineering, Beijing, China, Paper No. S28-004; 2008 (on CD).
[25] Panella, D. S., M. E. Tornello & C. D. Frau(2017). A simple an intuitive procedure to identify pulse-like ground motions. Soil Dynamics and Earthquake Engineering (94), 234-243.

Appendix 1. Ranking of pulse-like ground motions.

Complete list in http://www1.frm.utn.edu.ar/sismos/info_complementaria.php

Earthquake Name	Year	Magn. Mw	Station Name	Record Identification	IP	Dist. (km)
Northridge-01	1994	6,69	Newhall - W Pico Canyon Rd.	RSN1045_NORTHR_WPI046	6,5	2,1
Chi-Chi, Taiwan	1999	7,62	TCU068	RSN1505_CHICHI_TCU068-E	7,1	0,0
Imperial Valley-06	1979	6,53	El Centro Array #7	RSN182_IMPVALL.H_H-E07230	7,2	0,6
Chi-Chi, Taiwan	1999	7,62	TCU068	RSN1505_CHICHI_TCU068-N	7,4	0,0
Erzican, Turkey	1992	6,69	Erzincan	RSN821_ERZINCAN_ERZ-NS	7,5	0,0
Christchurch, New Zealand	2011	6,20	Christchurch Resthaven	RSN8119_CCHURCH_PRPCW	7,7	5,1
Imperial Valley-06	1979	6,53	El Centro - Meloland Geot. Array	RSN171_IMPVALL.H_H-EMO270	8,3	0,1
Loma Prieta	1989	6,93	Los Gatos - Lexington Dam	RSN3548_LOMAP_LEX090	8,8	3,2
San Salvador	1986	5,80	Geotech Investig Center	RSN568_SANSALV_GIC090	9	2,1
Kocaeli, Turkey	1999	7,51	Arcelik	RSN1148_KOCAELI_ARE090	9,1	10,6
Cape Mendocino	1992	7,01	Bunker Hill FAA	RSN3744_CAPEMEND_BNH270	9,3	8,5
Christchurch, New Zealand	2011	6,20	Christchurch Resthaven	RSN8119_CCHURCH_PRPCS	9,3	5,1
Imperial Valley-06	1979	6,53	El Centro - Meloland Geot. Array	RSN171_IMPVALL.H_H-EMO000	9,3	0,1
Imperial Valley-06	1979	6,53	El Centro Array #6	RSN181_IMPVALL.H_H-E06230	9,3	0,0
San Salvador	1986	5,80	Geotech Investig Center	RSN568_SANSALV_GIC180	9,3	2,1
Chi-Chi, Taiwan-03	1999	6,20	TCU076	RSN2627_CHICHI.03_TCU076E	9,6	13,0
Imperial Valley-06	1979	6,53	El Centro Array #4	RSN179_IMPVALL.H_H-E04230	9,7	4,9
Coyote Lake	1979	5,74	Gilroy Array #6	RSN150_COYOTELK_G06230	9,9	0,4
Chi-Chi, Taiwan	1999	7,62	TCU052	RSN1492_CHICHI_TCU052-N	10	0,0
Imperial Valley-06	1979	6,53	EC County Center FF	RSN170_IMPVALL.H_H-ECC092	10,1	7,3
Loma Prieta	1989	6,93	Los Gatos - Lexington Dam	RSN3548_LOMAP_LEX000	10,1	3,2
Northridge-01	1994	6,69	Pacoima Dam (downstr)	RSN1050_NORTHR_PAC175	10,3	4,9
Imperial Valley-06	1979	6,53	El Centro Array #5	RSN180_IMPVALL.H_H-E05230	10,4	1,8
San Salvador	1986	5,80	National Geografical Inst	RSN569_SANSALV_NGI180	10,4	3,7
San Salvador	1986	5,80	National Geografical Inst	RSN569_SANSALV_NGI270	10,8	3,7
Erzican, Turkey	1992	6,69	Erzincan	RSN821_ERZINCAN_ERZ-EW	10,9	0,0
Northridge-01	1994	6,69	Sylmar - Olive View Med FF	RSN1086_NORTHR_SYL360	10,9	1,7
Kobe, Japan	1995	6,90	Port Island (0 m)	RSN1114_KOBE_PRI000	11,2	3,3
Parkfield-02, CA	2004	6,00	Parkfield - Fault Zone 1	RSN4107_PARK2004_COW360	11,3	0,0
Superstition Hills-02	1987	6,54	Parachute Test Site	RSN723_SUPER.B_B-PTS225	11,3	1,0
Chi-Chi, Taiwan-03	1999	6,20	CHY080	RSN2495_CHICHI.03_CHY080E	11,5	21,3
Northridge-01	1994	6,69	Jensen Filter Plant Administrative Buil.	RSN982_NORTHR_JEN022	11,5	0,0
Cape Mendocino	1992	7,01	Cape Mendocino	RSN825_CAPEMEND_CPM000	11,6	0,0
Parkfield-02, CA	2004	6,00	Parkfield - Cholame 2WA	RSN4100_PARK2004_C02090	11,6	1,6
Friuli (aftershock 9), Italy	1976	5,50	Buia	RSN4276_FRIULI.P_W-BUI000	11,7	6,0
Coalinga-05	1983	5,77	Pleasant Valley P.P. - yard	RSN412_COALINGA_D-PVY045	11,8	13,2
Northridge-01	1994	6,69	Newhall - W Pico Canyon Rd.	RSN1045_NORTHR_WPI316	11,8	2,1
Cape Mendocino	1992	7,01	Ferndale Fire Station	RSN3748_CAPEMEND_FFS270	11,9	16,6
Kocaeli, Turkey	1999	7,51	Gebze	RSN1161_KOCAELI_GBZ000	11,9	7,6
Northridge-01	1994	6,69	LA Dam	RSN1013_NORTHR_LDM064	11,9	0,0
Parkfield-02, CA	2004	6,00	Parkfield - Cholame 1E	RSN4098_PARK2004_C01090	12	1,7
Chi-Chi, Taiwan	1999	7,62	TCU052	RSN1492_CHICHI_TCU052-E	12,1	0,0
Northridge-01	1994	6,69	Rinaldi Receiving Sta	RSN1063_NORTHR_RRS228	12,1	0,0
Parkfield-02, CA	2004	6,00	Parkfield - Cholame 1E	RSN4098_PARK2004_C01360	12,1	1,7
N. Palm Springs	1986	6,06	North Palm Springs	RSN529_PALMSPR_NPS210	12,3	0,0
Christchurch, New Zealand	2011	6,20	Styx Mill Transfer Station	RSN8130_CCHURCH_SHLCS50E	12,5	11,2
Imperial Valley-06	1979	6,53	El Centro Array #7	RSN182_IMPVALL.H_H-E07140	12,6	0,6
Cape Mendocino	1992	7,01	Bunker Hill FAA	RSN3744_CAPEMEND_BNH360	12,7	8,5
Spitak, Armenia	1988	6,77	Gukasian	RSN730_SPITAK_GUK000	12,7	24,0
Coyote Lake	1979	5,74	Gilroy Array #2	RSN147_COYOTELK_G02140	12,9	8,5
Northridge-01	1994	6,69	Sylmar - Converter Sta East	RSN1085_NORTHR_SCE011	13	0,0
Christchurch, New Zealand	2011	6,20	Kaiapoi North School	RSN8090_CCHURCH_HPSCS86W	13,2	17,9
Christchurch, New Zealand	2011	6,20	Styx Mill Transfer Station	RSN8130_CCHURCH_SHLCS40W	13,2	11,2
Chuetsu-oki	2007	6,80	Kashiwazaki City Center	RSN4856_CHUETSU_65025NS	13,2	0,0
N. Palm Springs	1986	6,06	Morongo Valley Fire Station	RSN527_PALMSPR_MVH135	13,2	3,6
Denali, Alaska	2002	7,90	TAPS Pump Station #10	RSN2114_DENALI_PS10-047	13,3	0,2

Earthquake Name	Year	Magn. Mw	Station Name	Record Identification	IP	Dist. (km)
Imperial Valley-06	1979	6,53	El Centro Differential Array	RSN184_IMPVALL.H_H-EDA270	13,3	5,1
Kalamata, Greece-01	1986	6,20	Kalamata (bsmt)	RSN564_GREECE_H-KAL-NS	13,3	6,5
Kobe, Japan	1995	6,90	Takarazuka	RSN1119_KOBE_TAZ090	13,3	0,0
Mt. Lewis	1986	5,60	Halls Valley	RSN502_MTLEWIS_HVR090	13,3	12,4
Parkfield-02, CA	2004	6,00	Slack Canyon	RSN4097_PARK2004_SCN360	13,3	1,6
Parkfield-02, CA	2004	6,00	Parkfield - Fault Zone 9	RSN4113_PARK2004_Z09090	13,3	1,2
Morgan Hill	1984	6,19	Coyote Lake Dam - Southwest Abut.	RSN451_MORGAN_CYC285	13,4	0,2
Imperial Valley-06	1979	6,53	Brawley Airport	RSN161_IMPVALL.H_H-BRA315	13,5	8,5
Kobe, Japan	1995	6,90	Kobe University	RSN1108_KOBE_KBU000	13,6	0,9
Imperial Valley-06	1979	6,53	El Centro Array #10	RSN173_IMPVALL.H_H-E10050	13,7	8,6
Parkfield-02, CA	2004	6,00	Parkfield - Fault Zone 12	RSN4115_PARK2004_PRK360	13,7	0,9
Chi-Chi, Taiwan	1999	7,62	TCU101	RSN1528_CHICHI_TCU101-E	13,8	2,1
Darfield, New Zealand	2010	7,00	SBRC	RSN6962_DARFIELD_ROLCS29E	13,8	21,3
Joshua Tree, CA	1992	6,10	North Palm Springs Fire Sta #36	RSN6877_JOSHUA_5294090	13,8	21,4
Kocaeli, Turkey	1999	7,51	Gebze	RSN1161_KOCAELI_GBZ270	13,8	7,6
Northridge-01	1994	6,69	Pacoima Dam (downstr)	RSN1050_NORTHR_PAC265	13,8	4,9
Chi-Chi, Taiwan-03	1999	6,20	TCU078	RSN2628_CHICHI.03_TCU078E	13,9	0,0
Imperial Valley-06	1979	6,53	Brawley Airport	RSN161_IMPVALL.H_H-BRA225	13,9	8,5
Loma Prieta	1989	6,93	Saratoga - W Valley Coll.	RSN803_LOMAP_WVC270	13,9	8,5
Coalinga-05	1983	5,77	Transmitter Hill	RSN415_COALINGA_D-TSM360	14,1	3,7
Coyote Lake	1979	5,74	Gilroy Array #3	RSN148_COYOTELK_G03140	14,1	6,8
Darfield, New Zealand	2010	7,00	Hulverstone Drive Pumping Station	RSN6911_DARFIELD_HORCN18E	14,3	25,4
Parkfield-02, CA	2004	6,00	Parkfield - Cholame 2WA	RSN4100_PARK2004_C02360	14,3	1,6
Whittier Narrows-01	1987	5,99	Downey - Birchdale	RSN614_WHITTIER.A_A-BIR180	14,3	14,9
Coalinga-05	1983	5,77	Pleasant Valley P.P. - FF	RSN411_COALINGA_D-PVP360	14,4	13,2
Kocaeli, Turkey	1999	7,51	Yarimca	RSN1176_KOCAELI_YPT150	14,4	1,4
Kocaeli, Turkey	1999	7,51	Duzce	RSN1158_KOCAELI_DZC180	14,5	13,6
Kocaeli, Turkey	1999	7,51	Duzce	RSN1158_KOCAELI_DZC270	14,5	13,6
Parkfield-02, CA	2004	6,00	Parkfield - Cholame 3W	RSN4102_PARK2004_C03360	14,5	2,6
Westmorland	1981	5,90	Parachute Test Site	RSN316_WESMORL_PTS225	14,6	16,5
Chi-Chi, Taiwan	1999	7,62	TCU103	RSN1530_CHICHI_TCU103-E	14,7	6,1
Chuetsu-oki	2007	6,80	Kashiwazaki City Center	RSN4856_CHUETSU_65025EW	14,7	0,0
Imperial Valley-06	1979	6,53	El Centro Array #6	RSN181_IMPVALL.H_H-E06140	14,7	0,0
Irpinia, Italy-01	1980	6,90	Sturno (STN)	RSN292_ITALY_A-STU270	14,7	6,8
Loma Prieta	1989	6,93	Gilroy - Historic Bldg.	RSN764_LOMAP_GOF160	14,7	10,3
Superstition Hills-02	1987	6,54	Kornbloom Road (temp)	RSN722_SUPER.B_B-KRN360	14,8	18,5
Northridge-01	1994	6,69	Pardee - SCE	RSN1054_NORTHR_PAR--L	14,9	5,5
Christchurch, New Zealand	2011	6,20	Kaiapoi North School	RSN8090_CCHURCH_HPSCN04W	15	17,9
Darfield, New Zealand	2010	7,00	LPCC	RSN6927_DARFIELD_LINCN23E	15	25,2
Northridge-01	1994	6,69	Sylmar - Olive View Med FF	RSN1086_NORTHR_SYL090	15	1,7
Chi-Chi, Taiwan	1999	7,62	TCU128	RSN1548_CHICHI_TCU128-E	15,1	13,1
Imperial Valley-06	1979	6,53	Holtville Post Office	RSN185_IMPVALL.H_H-HVP225	15,1	5,4
Christchurch, New Zealand	2011	6,20	Hulverstone Drive Pumping Station	RSN8067_CCHURCH_CMHSN10E	15,2	4,3
Imperial Valley-06	1979	6,53	Holtville Post Office	RSN185_IMPVALL.H_H-HVP315	15,3	5,4
Kocaeli, Turkey	1999	7,51	Yarimca	RSN1176_KOCAELI_YPT060	15,3	1,4
Chuetsu-oki	2007	6,80	Joetsu Kakizakiku Kakizaki	RSN4847_CHUETSU_65010EW	15,4	9,4
Parkfield-02, CA	2004	6,00	Parkfield - Cholame 4AW	RSN4104_PARK2004_C4A090	15,4	4,8
Coalinga-05	1983	5,77	Transmitter Hill	RSN415_COALINGA_D-TSM270	15,5	3,7
Parkfield-02, CA	2004	6,00	Parkfield - Cholame 3W	RSN4102_PARK2004_C03090	15,5	2,6
Chi-Chi, Taiwan-06	1999	6,30	TCU078	RSN3473_CHICHI.06_TCU078E	15,6	5,7
Imperial Valley-06	1979	6,53	El Centro Array #10	RSN173_IMPVALL.H_H-E10320	15,6	8,6
Parkfield-02, CA	2004	6,00	Parkfield - Fault Zone 1	RSN4107_PARK2004_COW090	15,6	0,0
Whittier Narrows-01	1987	5,99	Norwalk - Imp Hwy, S Grnd	RSN668_WHITTIER.A_A-NOR360	15,6	14,4
Livermore-01	1980	5,80	San Ramon - Eastman Kodak	RSN214_LIVERMOR_A-KOD180	15,7	15,2
Whittier Narrows-01	1987	5,99	Downey - Co Maint Bldg	RSN615_WHITTIER.A_A-DWN180	15,7	15,0
Chi-Chi, Taiwan-03	1999	6,20	TCU075	RSN2626_CHICHI.03_TCU075E	15,8	18,5

Earthquake Name	Year	Magn. Mw	Station Name	Record Identification	IP	Dist. (km)
Whittier Narrows-01	1987	5,99	LB - Orange Ave	RSN645_WHITTIER.A_A-OR2010	15,8	19,8
Parkfield-02, CA	2004	6,00	Parkfield - Fault Zone 6	RSN4110_PARK2004_Z06090	15,9	0,9
Parkfield-02, CA	2004	6,00	Parkfield - Stone Corral 1E	RSN4126_PARK2004_SC1360	15,9	2,9
Duzce, Turkey	1999	7,14	Duzce	RSN1605_DUZCE_DZC270	16	0,0
Chi-Chi, Taiwan	1999	7,62	TCU031	RSN1477_CHICHI_TCU031-E	16,1	30,2
Christchurch, New Zealand	2011	6,20	Riccarton High School	RSN8123_CCHURCH_REHSS88E	16,1	9,4
Christchurch, New Zealand	2011	6,20	SWNC	RSN8134_CCHURCH_SMTCN88W	16,1	25,5
Kobe, Japan	1995	6,90	Takarazuka	RSN1119_KOBE_TAZ000	16,1	0,0
Chi-Chi, Taiwan-03	1999	6,20	CHY028	RSN2461_CHICHI.03_CHY028E	16,2	23,4
Cape Mendocino	1992	7,01	Ferndale Fire Station	RSN3748_CAPEMEND_FFS360	16,3	16,6
Cape Mendocino	1992	7,01	Petrolia	RSN828_CAPEMEND_PET090	16,4	0,0
Northridge-01	1994	6,69	Jensen Filter Plant Administrative Building	RSN982_NORTHR_JEN292	16,4	0,0
Parkfield	1966	6,19	Temblor pre-1969	RSN33_PARKF_TMB205	16,4	16,0
Parkfield-02, CA	2004	6,00	PARKFIELD - MIDDLE MOUNTAIN	RSN4071_PARK2004_MIDDL360	16,4	0,6
Imperial Valley-06	1979	6,53	El Centro Array #8	RSN183_IMPVALL.H_H-E08140	16,5	3,9
Irpinia, Italy-01	1980	6,90	Bagnoli Irpinio	RSN285_ITALY_A-BAG270	16,5	8,1
Kobe, Japan	1995	6,90	Port Island (0 m)	RSN1114_KOBE_PRI090	16,5	3,3
Sierra Madre	1991	5,61	Altadena - Eaton Canyon	RSN1641_SMADRE_ALT000	16,5	8,6
Chi-Chi, Taiwan-03	1999	6,20	TCU122	RSN2655_CHICHI.03_TCU122E	16,6	18,1
Coyote Lake	1979	5,74	Gilroy Array #6	RSN150_COYOTELK_G06320	16,6	0,4
Imperial Valley-06	1979	6,53	Westmorland Fire Sta	RSN192_IMPVALL.H_H-WSM180	16,6	14,8
N. Palm Springs	1986	6,06	Morongo Valley Fire Station	RSN527_PALMSPR_MVH045	16,6	3,6
Northridge-01	1994	6,69	Newhall - Fire Sta	RSN1044_NORTHR_NWH360	16,6	3,2
Whittier Narrows-01	1987	5,99	Lakewood - Del Amo Blvd	RSN652_WHITTIER.A_A-DEL000	16,6	22,4
Imperial Valley-06	1979	6,53	El Centro Array #8	RSN183_IMPVALL.H_H-E08230	16,7	3,9
Nahanni, Canada	1985	6,76	Site 2	RSN496_NAHANNI_S2330	16,7	0,0
Chi-Chi, Taiwan	1999	7,62	TCU102	RSN1529_CHICHI_TCU102-E	16,8	1,5
Morgan Hill	1984	6,19	Gilroy Array #6	RSN459_MORGAN_G06090	16,8	9,9
Northridge-01	1994	6,69	Jensen Filter Plant Generator Building	RSN983_NORTHR_JGB022	16,8	0,0
Darfield, New Zealand	2010	7,00	HORC	RSN6906_DARFIELD_GDLCN55W	16,9	7,3
Northridge-01	1994	6,69	LA Dam	RSN1013_NORTHR_LDM334	16,9	0,0
Imperial Valley-06	1979	6,53	El Centro Array #3	RSN178_IMPVALL.H_H-E03230	17	10,8
Nahanni, Canada	1985	6,76	Site 2	RSN496_NAHANNI_S2240	17	0,0
Coyote Lake	1979	5,74	Gilroy Array #4	RSN149_COYOTELK_G04360	17,1	4,8
Chuetsu-oki	2007	6,80	Kashiwazaki NPP, S. Hall Array 2.4 m depth	RSN4896_CHUETSU_SG01EW	17,2	0,0
Mammoth Lakes-02	1980	5,69	Mammoth Lakes H. S.	RSN235_MAMMOTH.J_J-MLS254	17,2	1,5
Parkfield-02, CA	2004	6,00	PARKFIELD - MIDDLE MOUNTAIN	RSN4071_PARK2004_MIDDL-90	17,2	0,6
Chi-Chi, Taiwan	1999	7,62	TCU128	RSN1548_CHICHI_TCU128-N	17,3	13,1
Chi-Chi, Taiwan-03	1999	6,20	CHY028	RSN2461_CHICHI.03_CHY028N	17,3	23,4
Loma Prieta	1989	6,93	Hollister Differential Array	RSN778_LOMAP_HDA165	17,4	24,5
Parkfield-02, CA	2004	6,00	PARKFIELD - 1-STORY SCHOOL BLDG	RSN4084_PARK2004_36531003	17,4	1,0
Parkfield-02, CA	2004	6,00	Parkfield - Cholame 4W	RSN4103_PARK2004_C04360	17,4	3,3
Parkfield-02, CA	2004	6,00	Parkfield - Stone Corral 1E	RSN4126_PARK2004_SC1090	17,4	2,9
Christchurch, New Zealand	2011	6,20	Christchurch Hospital	RSN8064_CCHURCH_CCCCN64E	17,5	4,8
Christchurch, New Zealand	2011	6,20	Christchurch Cashmere High School	RSN8066_CCHURCH_CHHCN01W	17,5	4,4
Parkfield-02, CA	2004	6,00	Parkfield - Cholame 3E	RSN4101_PARK2004_TM3090	17,5	5,0
Chuetsu-oki	2007	6,80	NIG018	RSN5264_CHUETSU_NIG018NS	17,6	0,0
Imperial Valley-06	1979	6,53	Agrarias	RSN159_IMPVALL.H_H-AGR273	17,6	0,0
Cape Mendocino	1992	7,01	Centerville Beach, Naval Fac	RSN3746_CAPEMEND_CBF270	17,7	16,4
Christchurch, New Zealand	2011	6,20	Pages Road Pumping Station	RSN8118_CCHURCH_PPHSS57E	17,7	1,9
Northridge-01	1994	6,69	Pardee - SCE	RSN1054_NORTHR_PAR--T	17,7	5,5
Cape Mendocino	1992	7,01	Fortuna - Fortuna Blvd	RSN827_CAPEMEND_FOR000	17,8	16,0
Chi-Chi, Taiwan	1999	7,62	TCU063	RSN1501_CHICHI_TCU063-N	17,8	9,8
Chuetsu-oki	2007	6,80	Kashiwazaki NPP, S. Hall Array 2.4 m depth	RSN4896_CHUETSU_SG01NS	17,8	0,0
Imperial Valley-06	1979	6,53	Aeropuerto Mexicali	RSN158_IMPVALL.H_H-AEP045	17,8	0,0
Loma Prieta	1989	6,93	Saratoga - Aloha Ave	RSN802_LOMAP_STG090	17,8	7,6
Morgan Hill	1984	6,19	Coyote Lake Dam - Southwest Abutment	RSN451_MORGAN_CYC195	17,8	0,2
Morgan Hill	1984	6,19	Halls Valley	RSN461_MORGAN_HVR240	17,8	3,5

Earthquake Name	Year	Magn. Mw	Station Name	Record Identification	IP	Dist. (km)
Christchurch, New Zealand	2011	6,20	Christchurch Cathedral College	RSN8063_CCHURCH_CBGSS01W	17,9	3,2
Duzce, Turkey	1999	7,14	Bolu	RSN1602_DUZCE_BOL090	17,9	12,0
Northridge-01	1994	6,69	Pacoima Dam (upper left)	RSN1051_NORTHR_PUL194	17,9	4,9
Bam, Iran	2003	6,60	Bam	RSN4040_BAM_BAM-L	18	0,1
Umbria Marche (foreshock) It.	1997	5,70	Colfiorito	RSN4337_UBMARCHE.P_B-CLF270	18	0,6
Cape Mendocino	1992	7,01	Centerville Beach, Naval Fac	RSN3746_CAPEMEND_CBF360	18,2	16,4
Chi-Chi, Taiwan	1999	7,62	TCU064	RSN1502_CHICHI_TCU064-N	18,2	16,6
Kobe, Japan	1995	6,90	Takatori	RSN1120_KOBE_TAK090	18,2	1,5
Northridge-01	1994	6,69	Sylmar - Converter Sta	RSN1084_NORTHR_SCS052	18,2	0,0
Baja California	1987	5,50	Cerro Prieto	RSN585_BAJA_CPE251	18,3	3,4
Chi-Chi, Taiwan-03	1999	6,20	CHY024	RSN2457_CHICHI.03_CHY024E	18,3	18,5
Chi-Chi, Taiwan-03	1999	6,20	TCU116	RSN2650_CHICHI.03_TCU116E	18,3	21,1
Imperial Valley-06	1979	6,53	Westmorland Fire Sta	RSN192_IMPVALL.H_H-WSM090	18,3	14,8
Chi-Chi, Taiwan	1999	7,62	TCU040	RSN1483_CHICHI_TCU040-E	18,4	22,1
Chuetsu-oki	2007	6,80	Yoshikawaku Joetsu City	RSN4850_CHUETSU_65013NS	18,4	13,7
San Fernando	1971	6,61	Pacoima Dam (upper left abut)	RSN77_SFERN_PUL164	18,4	0,0
Chi-Chi, Taiwan	1999	7,62	TCU136	RSN1550_CHICHI_TCU136-N	18,6	8,3
Darfield, New Zealand	2010	7,00	HORC	RSN6906_DARFIELD_GDLCS35W	18,6	7,3
Parkfield-02, CA	2004	6,00	Parkfield - Cholame 4W	RSN4103_PARK2004_C04090	18,6	3,3
Parkfield-02, CA	2004	6,00	Parkfield - Vineyard Cany 1E	RSN4130_PARK2004_PV1090	18,6	1,6
Imperial Valley-06	1979	6,53	EC County Center FF	RSN170_IMPVALL.H_H-ECC002	18,8	7,3
Landers	1992	7,28	Lucerne	RSN879_LANDERS_LCN260	18,8	2,2
Chi-Chi, Taiwan	1999	7,62	TCU104	RSN1531_CHICHI_TCU104-N	18,9	12,9
Imperial Valley-06	1979	6,53	El Centro Array #3	RSN178_IMPVALL.H_H-E03140	18,9	10,8
Landers	1992	7,28	Yermo Fire Station	RSN900_LANDERS_YER270	18,9	23,6
Parkfield-02, CA	2004	6,00	Parkfield - Fault Zone 12	RSN4115_PARK2004_PRK090	18,9	0,9
Parkfield-02, CA	2004	6,00	Parkfield - Fault Zone 14	RSN4116_PARK2004_Z14090	18,9	8,5
Chi-Chi, Taiwan	1999	7,62	TCU036	RSN1480_CHICHI_TCU036-E	19,1	19,8
Northridge-01	1994	6,69	Sylmar - Converter Sta	RSN1084_NORTHR_SCS142	19,1	0,0
Parkfield-02, CA	2004	6,00	Parkfield - Cholame 3E	RSN4101_PARK2004_TM3360	19,1	5,0
Parkfield-02, CA	2004	6,00	Parkfield - Fault Zone 15	RSN4117_PARK2004_Z15090	19,1	0,8
Superstition Hills-02	1987	6,54	Parachute Test Site	RSN723_SUPER.B_B-PTS315	19,1	1,0
Whittier Narrows-01	1987	5,99	Compton - Castlegate St	RSN611_WHITTIER.A_A-CAS000	19,1	18,3
Chi-Chi, Taiwan-03	1999	6,20	TCU065	RSN2618_CHICHI.03_TCU065E	19,2	25,2
Christchurch, New Zealand	2011	6,20	Christchurch Cashmere High School	RSN8066_CCHURCH_CHHCS89W	19,2	4,4
Duzce, Turkey	1999	7,14	Duzce	RSN1605_DUZCE_DZC180	19,2	0,0
N. Palm Springs	1986	6,06	Whitewater Trout Farm	RSN540_PALMSPR_WWT180	19,2	0,0
Chi-Chi, Taiwan-03	1999	6,20	CHY080	RSN2495_CHICHI.03_CHY080N	19,3	21,3
Chi-Chi, Taiwan-03	1999	6,20	TCU138	RSN2661_CHICHI.03_TCU138W	19,3	21,1
Loma Prieta	1989	6,93	Gilroy - Gavilan Coll.	RSN763_LOMAP_GIL067	19,3	9,2
Northern Calif-03	1954	6,50	Ferndale City Hall	RSN20_NCALIF.FH_H-FRN044	19,3	26,7
Northridge-01	1994	6,69	Newhall - Fire Sta	RSN1044_NORTHR_NWH090	19,3	3,2
Parkfield-02, CA	2004	6,00	Parkfield - Cholame 2E	RSN4099_PARK2004_TM2090	19,4	3,2
Victoria, Mexico	1980	6,33	Chihuahua	RSN266_VICT_CHI102	19,4	18,5
Chi-Chi, Taiwan	1999	7,62	CHY101	RSN1244_CHICHI_CHY101-N	19,5	9,9
Northridge-01	1994	6,69	Sylmar - Converter Sta East	RSN1085_NORTHR_SCE281	19,5	0,0
Chi-Chi, Taiwan-06	1999	6,30	TCU078	RSN3473_CHICHI.06_TCU078N	19,6	5,7
Chuetsu-oki	2007	6,80	Kariwa	RSN4875_CHUETSU_65058EW	19,6	0,0
Iwate	2008	6,90	Kitakami Yanagiharach	RSN5810_IWATE_56362EW	19,6	16,4
Chi-Chi, Taiwan	1999	7,62	TCU087	RSN1519_CHICHI_TCU087-E	19,7	7,0
Chuetsu-oki	2007	6,80	NIG018	RSN5264_CHUETSU_NIG018EW	19,7	0,0
Denali, Alaska	2002	7,90	TAPS Pump Station #10	RSN2114_DENALI_PS10-317	19,7	0,2
Christchurch, New Zealand	2011	6,20	Hulverstone Drive Pumping Station	RSN8067_CCHURCH_CMHSS80E	19,8	4,3
Northridge-01	1994	6,69	LA - Chalon Rd	RSN989_NORTHR_CHL160	19,8	9,9
Darfield, New Zealand	2010	7,00	WSFC	RSN6975_DARFIELD_TPLCN27W	19,9	24,4
Imperial Valley-06	1979	6,53	El Centro Array #5	RSN180_IMPVALL.H_H-E05140	19,9	1,8
Northwest China-03	1997	6,10	Jiashi	RSN1752_NWCHINA3_JIA270	19,9	10,0
Chi-Chi, Taiwan	1999	7,62	TCU075	RSN1510_CHICHI_TCU075-E	20	0,9
Loma Prieta	1989	6,93	Gilroy Array #1	RSN765_LOMAP_G01000	20	8,8